TABLE 3. Best Fit Statistical Distributions to Global Reflectivity Data

Distribution	Parameters	Mean for Fit	Standard Deviation For Fit	Correlation of Fit to Data (R^2)
Data	global data set	0.13	0.057	—
Gaussian	$\mu = 0.13$; $\sigma = 0.055$	0.132	0.055	0.92
Two-stage Gaussian*	$\mu_1 = 0.11$, $\sigma_1 = 0.026$, $\mu_2 = 0.14$, $\sigma_2 = 0.035$	0.126	0.047	0.98
Rayleigh	$\sigma = 0.104$	0.129	0.04	0.87
Log-hyperbolic	$\phi = 1.94$, $\gamma = -4.84$†	0.129	0.047	0.98

Equations for the distributions listed above in the form $f(x;$ parameters); Gaussian, $f(x; \mu, \sigma) = [1/\sigma(2\pi)^{1/2}] \exp\{-\frac{1}{2}[(x-\mu)/\sigma]^2\}$; two-stage Gaussian, $f(x; \mu_1, \mu_2, \sigma_1, \sigma_2) = [1/\sigma_1(2\pi)^{1/2}] \exp\{-\frac{1}{2}[(x-\mu_1)/\sigma_1]^2\} + [1/\sigma_2(2\pi)^{1/2}] \exp\{-\frac{1}{2}[(x-\mu_2)/\sigma_2]^2\}$; Rayleigh, $f(x; \sigma) = (x/\sigma^2) \exp[-\frac{1}{2}(x/\sigma)^2]$; log-hyperbolic, $f(x; \alpha, \delta, \beta, \mu, \phi, \gamma) = -\alpha[\delta^2 + (x-\mu)^2]^{1/2} + \beta(x-\mu) - \ln K(\delta, \gamma, \phi)$, where $K(\delta, \gamma, \phi)$ is a Bessel function of the third kind K_1 $[\delta(\gamma\phi)^{1/2}]$ times $[(1/\phi) + (1/\gamma)]$ $\delta(\gamma\phi)^{1/2}$ and ϕ, γ are the slopes of the two asymptotes for the hyperbola [*Bagnold and Barndorff-Nielsen*, 1980].

*Two independent Gaussian distributions added together with means μ_1, μ_2 and deviations σ_1, σ_2.

†Other parameter values for log-hyperbolic are $\alpha = 3.4$, $\delta = 0.06$, $\mu = -0.89$, $\beta = -1.5$, $\theta = 39°$ (angle between the two asymptotes).

rms slope (roughness) where two fundamental types of surfaces were identified [*Garvin et al.*, 1984*c*]. Table 3 summarizes the different types of statistical distributions which were fit to the ρ data. None was a significant improvement over the two-component Gaussian, although the log-hyperbolic [*Bagnold and Barndorff-Nielson*, 1980] was equally good, as is to be expected given its extreme versatility (e.g., six parameters). The geologic consequences of the different types of statistical fits which model the ρ data have not yet been fully explored, but the generally Gaussian nature (e.g., well behaved or consistent) of the data is worthy of note.

Almost 70% of the planet are in the 0.10–0.20 ρ interval where bedrock surfaces are likely to be common. Of the rest, 15% is less than 0.10 and 15% is greater than 0.20. This "inequity" in the ρ distribution is caused by the dominance of the rolling plains on Venus, which generally have values in the range 0.10–0.20. We will remove this weighting effect when ρ is correlated with elevation in a forthcoming section. Figure 2*b* shows the cumulative distribution of ρ on Venus. The ranges of the ρ values for the terrains investigated by the Venera landers are also shown. The horizontal bars represent 1σ and the central "dot" is the mean for those regions 200 × 200 km about the specified landing coordinates [*Garvin et al.*, 1984*a*, *c*]. Such areas represent the approximate landing error regions. The Venera 10 gamma ray spectrometer value corresponds to a bulk density of 2.8 g/cm^3, and the radar ρ value was computed using equation (11) in inverted form [*Keldysh*, 1979]. The apparent discrepancy between the surface density measurement ($\gamma = 2.8$ g/cm^3 gives $\rho = 0.17$), and the average radar ρ properties for the landing region ($\rho = 0.10$ gives $\gamma = 2.1$ g/cm^3) can be explained in terms of the observed extent of the soil cover on the bedrock. The gamma ray densitometer measured bedrock, while the soil deposits visible throughout the local area and surrounding region probably serve to lower the radar ρ as a result of their relatively large abundance. The Veneras did not sample either the soil-dominated or the high dielectric enriched surfaces that occur on Venus. None of the landers came to rest on those Venusian surfaces most like the moon in terms of their radar reflectivities or dielectric properties.

The Venus average ρ is within the range accepted for rock-dominated surfaces [*Evans and Hagfors*, 1968, and others], and the high ρ regions are apparently unique to Venus, at least in comparison with the moon and Mars. It is clear that there are few regions totally covered with highly porous materials. This suggests that either the processes available for making fine materials on Venus are not very effective (e.g., impact cratering, pyroclastic volcanism, mechanical and chemical weathering) or that there are processes capable of cementing, lithifying, or compacting porous materials enough to raise their radar ρ signatures appreciably. It is quite probable that weathering rates (at least in the plains) are low [*McGill et al.*, 1983], that mechanical abrasion is almost insignificant, and that some interparticle cementation does occur. As the distribution of ρ does not depend on latitude or on spatial associations with highlands, an examination of the correlation of ρ with elevation is warranted.

CORRELATION OF REFLECTIVITY AND ELEVATION

The PV reflectivity and elevation data sets have been corre lated by means of a three-dimensional scatter diagram (Figure 3); this approach was used by *Basilevsky et al.* [1982] in their analyses of roughness, topographic slope, and elevation for various distinct regions (e.g., Beta and Ishtar). *Garvin et al.* [1983, 1984*b*] used this technique when they correlated the global roughness data for Venus with elevation. The elevation and ρ spectra for Venus have been subdivided into 256 equally sized intervals (57 m and 0.002, respectively) for display and

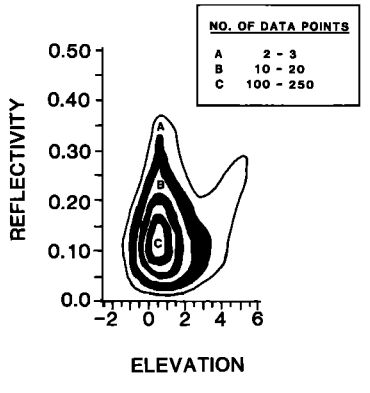

Fig. 3. Scatter diagram of reflectivity (vertical axis) versus elevation (horizontal axis, in kilometers relative to 6051). General trend of data density is shown in key. Detailed contours are as follows: A, 2-3; solid area, 4-9; B, 10-20; solid area, 21-99; white, 10-20; solid area, 21-99; C, 100-250.